

High-pressure highly reduced nitrides and oxides from chromitite of a Tibetan ophiolite

Larissa F. Dobrzhinetskaya^{a,1}, Richard Wirth^b, Jingsui Yang^c, Ian D. Hutcheon^d, Peter K. Weber^d, and Harry W. Green II^a

^aInstitute of Geophysics and Planetary Physics and Department of Earth Sciences, University of California, Riverside, CA 92521; ^bGeoForschungsZentrum, D-14473 Potsdam, Germany; ^cKey Laboratory for Continental Dynamics, Institute of Geology, Beijing 100037, China; and ^dGlenn T. Seaborg Institute, Lawrence Livermore National Laboratory, Livermore, CA 94551

Edited by Ho-kwang Mao, Carnegie Institution of Washington, Washington, DC, and approved September 25, 2009 (received for review May 21, 2009)

The deepest rocks known from within Earth are fragments of normal mantle (~400 km) and metamorphosed sediments (~350 km), both found exhumed in continental collision terranes. Here, we report fragments of a highly reduced deep mantle environment from at least 300 km, perhaps very much more, extracted from chromite of a Tibetan ophiolite. The sample consists, in part, of diamond, coesite-after-stishovite, the high-pressure form of TiO₂, native iron, high-pressure nitrides with a deep mantle isotopic signature, and associated SiC. This appears to be a natural example of the recently discovered disproportionation of Fe²⁺ at very high pressure and consequent low oxygen fugacity (fO₂) in deep Earth. Encapsulation within chromitite enclosed within upwelling solid mantle rock appears to be the only vehicle capable of transporting these phases and preserving their low-fO₂ environment at the very high temperatures of oceanic spreading centers.

boron nitride | coesite after stishovite | Luobasa chromitite | TiO₂ II | titanium nitride-osbornite

Until recently, the deepest rock samples recovered from Earth's interior were xenoliths carried to the surface in explosive eruptions of kimberlite and related rocks, with maximum depth of ~300 km (1). However, the advent of microstructural analysis of rocks from continental collision zones has established exhumation from still greater depths [peridotites from >300–400 km (2–5) and metamorphosed sediments from ~350 km (6)]. More recently, a small fraction of diamonds from kimberlitic rocks has been found to carry inclusions that strongly suggest even greater depths, perhaps 1,700 km (7), but rocks that previously incorporated those diamonds at depth have not been recognized. We report here discovery of unexpected mineral assemblages from an ocean-spreading center environment, representing another window into Earth's deep interior.

The discovery consists of very high-pressure and highly reduced phases extracted from chromitite within the mantle portion of an only lightly altered (e.g., small amounts of serpentine) fossil cross-section of oceanic crust and uppermost mantle (an ophiolite) in Tibet. Initial description of this material (8) documented diamonds and coesite-after-stishovite, establishing a minimum depth of origin of ~300 km. This surprising and curious discovery was strengthened by observation of coesite and diopside lamellae within chromite collected from the same outcrop (9) and, very importantly, discovery of diamonds and indicators of very low oxygen fugacity from similar chromitite in a second ophiolite in the Polar Ural Mountains (10), establishing that the Tibetan occurrence is not unique. This discovery strongly enhances the conclusion of ref. 8 that this occurrence of very high-pressure minerals is not the result of meteorite impact. Thus, a subset of ophiolites (currently of unknown abundance) contains high-pressure and reduced phases, despite the overwhelming evidence that the ophiolites themselves formed at oceanic spreading centers under oxidizing conditions.

Ophiolites typically consist of a crudely layered sequence of deep-water sediments, pillow-basalts, sheeted dikes, layered gabbros, and ultramafic rocks, all overlying common mantle rock

(harzburgite). The harzburgite is in all cases highly deformed in the solid state and almost universally contains rootless bodies of chromite ore for which the chromium content is always higher in chromitite than distributed within the harzburgite. Abundant evidence shows that modification of the chromite deposits takes place at shallow depths and not necessarily at the site of formation (11). Indeed, traditionally, chromite ores also have been considered to form at shallow mantle depths (e.g., ref. 11) and typically researchers have attributed the diamonds of Luobusa to come from no deeper than 150–200 km (e.g., ref. 12). The material that makes up the subject of both ref. 8 and this article has been extracted from massive chromite ore 93 of the Luobusa ophiolite, located on the collisional boundary between Asia and India (13, 14).

Results and Discussion

Terrestrial Nitrides and Single Crystals TiO₂ II as Inclusions in Coesite.

We now report high-pressure nitrides, oxides, and native Fe occurring as submicroscopic inclusions (50–200 nm) within coesite from the small rock fragment of ref. 8 (Fig. 1). The prismatic external form of the polycrystalline coesite domains that host these inclusions establish that the coesite formed by pseudomorphic replacement of stishovite (minimum pressure for its stability ~10 GPa, implying >300-km depth) (8). With a focused ion beam (FIB) instrument, we prepared several thin foils from this material that were examined in the transmission electron microscope (TEM), leading to discovery and characterization of the additional phases. Further analysis by nanometer-scale secondary ion mass spectrometry (NanoSIMS) determined the N and C isotopic compositions.

At the scale of the TEM, titanium nitride (TiN) is abundant within coesite and is accompanied by cubic boron nitride (c-BN) (Fig. 2*A* and *B*) and less-abundant crystals of native Fe (Fig. 2*C*) and sporadic inclusions of TiO₂ II (Fig. 2*E*), a high-pressure polymorph of rutile with the α PbO₂ structure (Fig. 2*F*) (15), and boron carbide of unknown stoichiometry. Electron diffraction analysis established the cubic symmetry of both nitrides, with $a = 4.23 \text{ \AA}$ for TiN (Fig. 2*D*) and $a = 3.61 \text{ \AA}$ for BN (Fig. 2*B*). TiO₂ II unit cell parameters were: $a = 4.49 \text{ \AA}$, $b = 5.47 \text{ \AA}$, $c = 4.91 \text{ \AA}$ (Fig. 2*F*). Initial identification of nitrides was accomplished by X-ray energy dispersive spectroscopy (EDS) but overlapping peaks of N K-peak and Ti K _{α} and K _{β} peaks, and N K-peak and B-K peak in this region of the spectrum, make such analysis qualitative at best. As a consequence, we analyzed both TiN and BN with electron energy loss spectroscopy (EELS) in the TEM and confirmed the identifications (Fig. 3). The EELS analysis confirms the 1:1 atomic ratio of both TiN and BN. Element

Author contributions: L.F.D. and J.Y. designed research; L.F.D., R.W., I.D.H., and P.K.W. performed research; L.F.D., R.W., I.D.H., and P.K.W. contributed new reagents/analytic tools; L.F.D., R.W., J.Y., I.D.H., P.K.W., and H.W.G. analyzed data; and L.F.D. and H.W.G. wrote the paper.

The authors declare no conflict of interest.

This article is a PNAS Direct Submission.

¹To whom correspondence should be addressed. E-mail: larissa@ucr.edu.

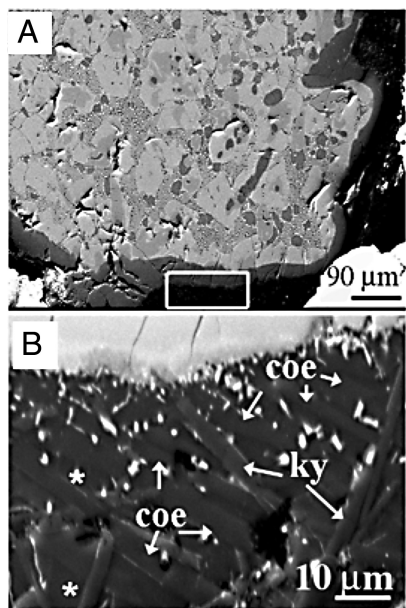


Fig. 1. Electron microscope images of studied sample. (A) Back-scattered electron image of Fe-Ti pellet rimmed by silicate rock (boxed area). (B) Detail of region within boxed area shows silicate material containing coesite (coe), kyanite (ky), unknown amorphous phase (*) of the following composition: [(wt. %) SiO₂ = 63.00, Al₂O₃ = 14.50, TiO₂ = 9.02, CaO = 0.5, MgO = 4.26, K₂O = 5.16] and Ti-rich minute phases (bright spots). Between metallic pellet and silicate rock there is a reaction zone (gray color at the top) containing in addition to Fe and Ti traces of Si and Al. See ref. 8 for additional images and detailed descriptions.

mapping showed that Ti, B and N are restricted to the nanoinclusions, whereas Si and O characterize the host coesite (Fig. 4).

Using a ≈ 100 -nm-diameter Cs⁺ primary beam, the isotopic compositions of N and C were measured by NanoSIMS on these same foils; the elemental distributions of N, C, and Si were also determined. A comparison of TEM images with NanoSIMS ¹²C¹⁴N isotope maps (nitrogen is detected as the CN molecule) demonstrates that TiN and c-BN are the only phases containing significant nitrogen (Fig. 5). With the exception of rare small (<50 nm) boron carbide grains intergrown with TiN and BN, carbon is much less abundant than nitrogen; it is found primarily as solid solution in TiN. Four replicate analyses of the largest available region of TiN ($\approx 2 \times 8 \mu\text{m}$) yielded isotopic compositions of $\delta^{15}\text{N} = -10.4 \pm 3.0\text{‰}$ and $\delta^{13}\text{C} = 5 \pm 7\text{‰}$; uncertainties are two standard errors. No variations in N and C isotope compositions were detected outside analytical uncertainty. The large uncertainty in $\delta^{13}\text{C}$ reflects the very small amount of C in the TiN and consequent low number of C ions collected.

Natural osbornite (TiN) is very rare on Earth (16, 17) and has never been found in situ; it is reasonably common in meteorites, especially iron meteorites (18). However, neither boron nitride nor boron carbide have previously been found in nature. TiO₂ II has been reported from two terrestrial localities (19, 20); in both cases it is preserved only in a special low-energy environment along a single twin boundary of a retrograde rutile crystal. Here, we found it as isolated crystals with no evidence of reversion to rutile. The presence of TiO₂ II, by itself, confirms the 10-GPa minimum pressure necessary to stabilize stishovite because at 1,300 °C, certainly a minimum temperature for a mantle upwelling at 300 km, rutile is stable to 10 GPa (15).

Low Oxygen Fugacity (fO₂) in the Loubasa Chromite. Another perplexing aspect of this problem is the very low fO₂ conditions of

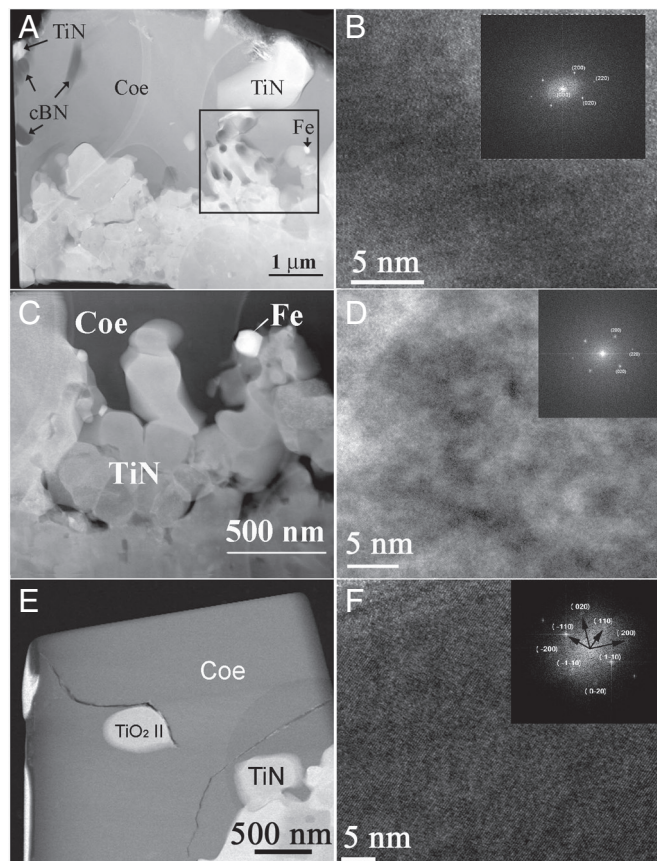


Fig. 2. TEM bright-field images of FIB-prepared foils. (A) The upper part of the foil is occupied by coesite (light gray contrast) containing nanometric inclusions of TiN, cBN, and native Fe; the boxed area shows intergrown TiN (bright) and cBN (dark gray) within coesite (medium gray). A small grain of native Fe (very bright) is shown at right. (B) Electron diffraction patterns of cBN. (C) An adjacent region of the foil contains equant crystals of TiN included in coesite. (D) Electron diffraction patterns of TiN. (E) A single crystal of TiO₂ II is included in coesite; at the lower right corner there is an inclusion of TiN. The bright stripes in the left side of the plate are a film of gallium deposited during foil preparation with FIB. (F) Electron diffraction patterns of TiO₂ II.

these materials, including SiC (12), although the latter is not incorporated in this particular specimen. Recent experimental work has shown that, under conditions of the lower mantle (21, 22) and even deep upper mantle (23), ferrous ion disproportionates into ferric ion + Fe metal. Thus, it may be that only the outermost shell of Earth [perhaps as thin as ≈ 250 km (23)] is strongly oxidized and that it should be expected that rocks/minerals brought to shallow levels from great depth could arrive highly reduced if protected during their last few hundred kilometers of travel. In the case under discussion here, the abundant evidence for shallow mantle processes active at higher fO₂ in this and other ophiolites means that the reduced conditions recorded in the sample discussed here had to be preserved by shielding from the shallow environment by encapsulation within chromite. That this could occur at the very high temperatures characteristic of oceanic spreading environments is surprising.

The Luobusa chromites provide information that is consistent with this hypothesis. The chromite of the massive deposit that carries the signal of very low fO₂ (including the presence of native Fe), shows a high Fe³⁺/ΣFe = 39 ± 1%, whereas it is Fe³⁺/ΣFe = 21 ± 1% in the disseminated ore that clearly has been affected by shallow processes. The electron microprobe chemical analyses revealed the following composition of chromites hosting the exotic inclusions described herein: (*n* = 3,

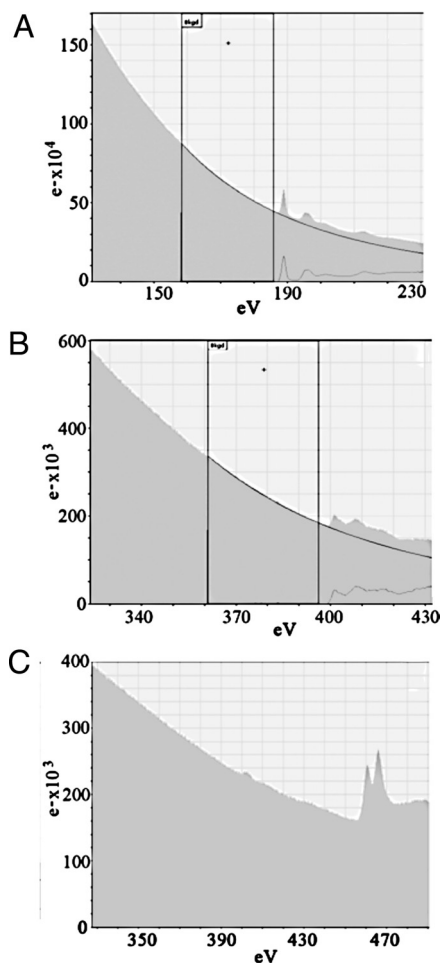


Fig. 3. EELS spectra acquired from cBN. (A) Shown is the boron K-edge between 189 and 197 eV. (B) Shown is the nitrogen K-edge situated between 400 and 405 eV. The spectra of A and B were collected from the spot within the cBN in the boxed area of Fig. 2A, confirming the presence of BN. (C) Shown is the EELS spectrum of TiN measured in the boxed area of Fig. 2A. The nitrogen-K edge is situated between 400 and 405 eV, and two sharp peaks at 455–475 eV are characteristic of the Ti L_{3,2} edge. No K edge for oxygen is present, confirming, therefore, the composition TiN.

wt%) MgO = 15.62, Al₂O₃ = 11.04, TiO₂ = 0.16, Cr₂O₃ = 60.43, Σ FeO = 12.10, NiO = 0.18, total = 99.53. Mossbauer data collected by T. Ruskov (Institute for Nuclear Research and Nuclear Energy, Sofia, Bulgaria) from the same chromite grains yield $Fe^{3+}/\Sigma Fe = 39 \pm 1\%$; the calculated chemical formula of chromite is $(Fe^{+2}_{0.18}Fe^{+3}_{0.08}Mg^{+2}_{0.74})_{1.0}(Cr_{1.51}Al_{0.41}Ti_{0.01}Fe^{+3}_{0.05})_{1.98}O_4$. On the one hand, because this chromite contains a high fraction of Fe³⁺, by conventional interpretation it implies a highly oxidized environment. However, this Fe³⁺-rich chromite contains Fe⁰ (native Fe) and other metals and highly reduced metal nitrides that are stable at high pressures and high temperatures (24, 25) and show no evidence of low T alteration (Fig. 2A and B). It also contains inclusions of the ultrahigh-pressure (UHP) phases TiO₂ II (described herein) and exsolution lamellae of coesite and diopside (9), suggesting that a precursor of such chromite could be a high-pressure polymorph of chromite (26). Given the totality of these observations, we suggest that the resolution of conflicting fO₂ indicators is that in the deep mantle (>300 km) the fO₂ is low and the elevated abundance of Fe³⁺ is a consequence of crystallographic constraints imposed by high-pressure host phases. Upon decompression and stabilization of upper-mantle minerals with abundant Fe²⁺ sites, the Fe³⁺

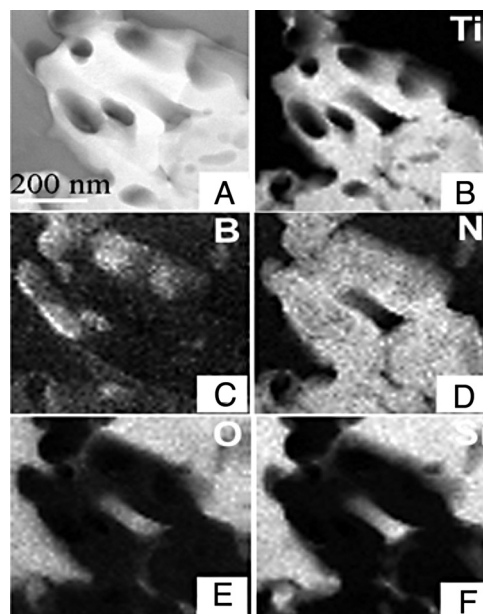


Fig. 4. EDS element maps of the area boxed in Fig. 2A. (A) Bright-field image of the mapped area. (B–F) Distribution of titanium (B), boron (C), nitrogen (D), oxygen (E), and silicon (F), confirming the presence of both boron and titanium nitrides inclusions in coesite. Nitrogen and boron were also confirmed with EELS.

and Fe⁰ react in the reverse direction of the Fe²⁺ disproportionation proposed by (21)



and, if all Fe⁰ is consumed, the fO₂ rises to the observed values of the upper mantle. In the present case, this reaction took place

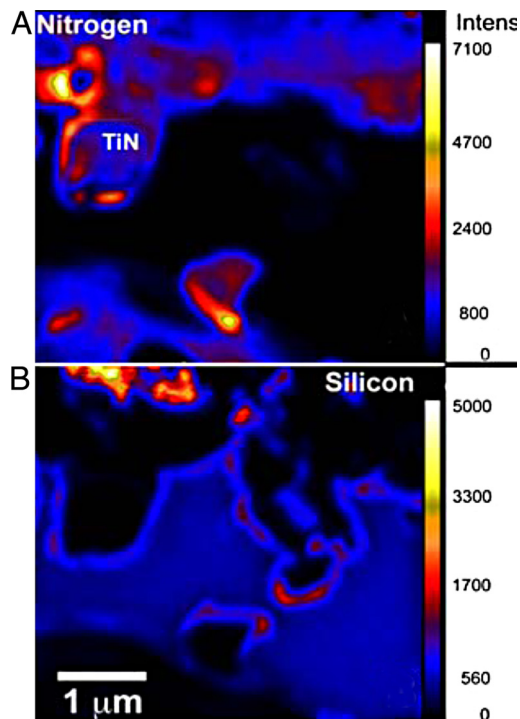


Fig. 5. Nitrogen (A) and silicon (B) element maps of the TEM foil acquired by NanoSIMS. The intensities of the elements are shown by the color barscale.

outside of chromite but the low fO_2 was preserved within massive chromite because of the abundant reduced phases within a highly restricted, refractory, chemical environment.

Our Mössbauer studies result looks exactly like the disproportionation of Fe^{2+} in the experiments discussed above, suggesting that at some time in the early history of the chromitite, perhaps in the stability field of a high-pressure polymorph, crystallographic constraints on the number of Fe^{3+} sites in the chromite polymorph have simultaneously increased the abundance of ferric iron and stabilized native iron, dropping the overall oxygen fugacity. If so, these rocks may be the first recognized natural example that the deep mantle may be characterized by phases that enforce disproportionation of Fe^{2+} and low fO_2 . Upwelling of such rocks to the surface where ferrous sites are abundant and ferric sites rare in mantle phases would lead to oxidation except in rare cases, such as this one, where local isolation has retained the low fO_2 and consequently the deep mantle phases. Detailed examination of chromitites worldwide and high-pressure experimentation on Cr-rich systems are both required to address these possibilities.

In addition to these indicators suggestive of very high pressure, the exsolution lamellae of coesite and diopside from chromite (9) show that at some time in the history of this deposit both SiO_2 and $CaMgSi_2O_6$ were soluble to a significant extent in chromite or its predecessor. The knowledge that chromite bulk chemistry can be stable to >20 GPa through at least two high-pressure polymorphs (26), and the experimental demonstration that the SiO_2 solubility in spinel-structured phases increases greatly at very high pressures (27), are consistent with the hypothesis that at least part of the massive chromite ore at Luobusa has a very deep origin and its refractory nature has shielded relics of such depths from obliteration by shallow processes.

How Great Might the Depth of Origin Be? We can set a minimum depth of 300 km for the origin of this material through the presence of TiO_2 II and former presence of stishovite, but we cannot yet constrain the maximum depth. For example, the upper limit of stishovite stability is ≈ 80 GPa (28); TiN is stable to at least 40 GPa (24) and c-BN to at least 60 GPa (25, 29). Kyanite is stable only to ≈ 15 GPa, where it breaks down to corundum + stishovite (30), but the reverse reaction could have accompanied decompression events, similar to stishovite inversion to coesite. Chromite is stable only to 12 GPa, but chromite stoichiometry is stable to at least 20 GPa (26). Thus, the origin of these materials can have been either from the deep upper mantle or the lower mantle.

Geophysical Significance of Nitrides and Related UHP Phases. In attempting to understand these observations in greater detail, two major questions remain: What is the significance that this finding of nitrides and other UHP minerals in mantle rocks occurs in a zone of upwelling; especially, where does the N come from? How can coesite and TiO_2 II be preserved within these high-temperature rocks with absolutely no evidence of reaction to their low-pressure polymorphs, quartz and rutile, respectively?

The geological setting of the host ophiolite strongly suggests nitrogen in the nanoinclusions is mantle-derived. The systematics of N isotope distribution in Earth are complex but most upper-mantle rocks exhibit a consistent signature of $\delta^{15}N = -5 \pm 2\text{‰}$, implying a globally uniform reservoir (31). Exceptions to this uniformity are sporadic much more negative values, e.g., $\delta^{15}N = -25\text{‰}$ in Fuxian diamonds (32) and $\delta^{15}N$ as low as -24‰ for some mid-ocean ridge basalt (MORB) samples (33). In contrast to these negative values from the mantle, the atmosphere, ocean, and crust are all characterized by positive values of $\delta^{15}N$: 0 – $+5\text{‰}$ for the atmosphere and ocean and $+5$ – $+12\text{‰}$ for the crust (granites, metamorphic rocks, and

sediments) (31). It has been recently found that ocean island basalt magmas thought to come from the bottom of the upper mantle or the lower mantle have $\delta^{15}N$ values in the same range as continental materials (31). Similarly, a study of SiC in kimberlites of Russian Siberia (34) found crustal values of $\delta^{15}N$ and highly negative values of $\delta^{13}C$. Both of these observations suggest N from subducted continental material and the C isotopes are consistent with subducted organic carbon.

Our isotopic results, with $\delta^{15}N = -10 \pm 3\text{‰}$, are inconsistent with a continental origin for the N, despite the fact that the material discussed here (rich in SiO_2 and Al_2O_3 and carrying boron and some alkalis) is chemically incompatible with mantle rocks, at least at pressures within the upper mantle, thereby suggesting an origin from subducted continental material or oceanic sediments. The $\delta^{15}N$ results are slightly more negative than most uppermost mantle N, but they are in the same direction as other, more negative, outliers. We conclude that this is mantle N, perhaps from an old and/or deep mantle reservoir. There is intriguing literature addressing the possibilities for N incorporation into the deep Earth as nitrides. It includes finding ilmenite xenocrysts in an African kimberlite containing 2.5 wt% N in their structure (35) (or, given our results, perhaps as included nitrides), a hypothetical prediction that TiN should be a mantle phase that binds nitrogen “missing” after Earth accretion (33), and synthesis of Fe-nitrides at extreme pressures and temperatures as a possible candidate for light element participation in formation of the core (36). The results of this study support the concept of deep nitrides and suggest that the source is not caused by recycling from the surface. They also suggest that other materials showing evidence of origin from great depths deserve systematic testing for N. A focus on the role of nitrogen might bring unexpected developments in understanding of our planet’s history.

Our carbon isotopic results ($\delta^{13}C = 5 \pm 7\text{‰}$) are nominally high for normal mantle C, but the large statistical error in the numbers makes it impossible to argue for significance of this observation. However, our results are clearly inconsistent with the strongly negative values of subducted organic carbon, leaving us with an inconsistency between the major element chemistry (and boron) of this rock fragment (that simple logic would suggest is continental in nature) and the volatile content. Either there is a way to explain the SiO_2 - and Al_2O_3 -rich, B- and alkali-bearing bulk chemistry as being compatible with a mantle origin, or we must conclude that the volatiles were added later in the history of this rock. Significantly more negative values found, e.g., in diamonds from Fuxian, China ($\delta^{15}N = -25\text{‰}$) (32) and sporadic similar values reported from MORB (33, 37) suggest there is a reservoir at greater depth with more negative $\delta^{15}N$ values that also could be the explanation for our data. How such N could get into this material depends strongly on how deep is the origin of the host chromitites and what is the origin of the extremely low fO_2 within them.

Last, how can one explain the unaltered state of coesite and TiO_2 II at low pressure and high temperature? At temperatures appropriate for mantle upwelling at ocean spreading centers, TiO_2 II is stable only at pressures within the stishovite stability field (>10 GPa) (15). Nevertheless, neither the TiO_2 II nanoinclusions nor the host coesite show any evidence of reaction to their low-pressure polymorphs, rutile and quartz, respectively. These observations contrast sharply with the observation that in UHP rocks from continental collision zones; relict coesite is heavily reacted to quartz and TiO_2 II is restricted to low-energy sites along rutile twin boundaries (19, 20). Preservation in such a pristine state in this ophiolite must reflect an extraordinarily low local f_{H_2O} , which is consistent with the very low fO_2 indicated by the coexisting phases.

Summary. The observations reported here show that nitrides, oxides, and metals encapsulated within massive chromite of an ophiolite carry a record of formation at very high pressure and temperature and very low fO_2 . Given that these materials came to near the surface at a temperature $\approx 1,300^\circ\text{C}$, they must have been at least that hot at their depth of formation, $>300\text{ km}$ (pressure $>10\text{ GPa}$). Although we still lack a full explanation of these findings, the fact that chromite of a second ophiolite also has been found to contain abundant diamonds and other exotic, reduced phases (10) verifies that chromite inclusions of at least some ophiolites offer another window into the deep mantle and the distribution of nitrogen in Earth.

Methods and Analytical Techniques

FIB Sample Preparation. Electron transparent foils were prepared with the FIB instrument (FEI FIB200) from selected areas. The foils were milled normal to the surface of the carbon-coated thin section, thereby excluding any surface contamination of the TEM foil. The foil was $\approx 15 \times 10 \times 0.150\ \mu\text{m}$. Details of the FIB method are in ref. 38.

TEM. TEM investigations were performed with a TECNAI F20 XTWIN TEM operating at 200 kV with a field emission electron source. The TEM is equipped with a Gatan Tridiem filter, an EDAX Genesis X-ray analyzer with ultra-thin window, and a Fishione high-angle annular dark-field detector. Tridiem filter was used for the acquisition of energy-filtered images, applying a 20-eV window to the zero loss peak. EELS spectra were acquired with a dispersion of 0.1 eV/channel and an entrance aperture of 2 mm. The resolution of the filter was 0.9 eV at half-width, at full maximum of the zero loss peak. Spectra were acquired in the diffraction mode. Acquisition time was 1 s. Spectra processing (background subtraction, removal of plural scattering) was performed by using the DigitalMicrograph software package. EDS spectra were usually acquired in the scanning transmission mode by using the TIA software package of the TEM. Significant mass loss during analysis was avoided by scanning the beam in a preselected window (according to the size of the measured volume). Spot size was $\approx 1\text{ nm}$, and acquisition time was 60 s.

NanoSIMS. SIMS of FIB sections was performed at the Lawrence Livermore National Laboratory by using a Cameca NanoSIMS 50 instrument. A $\approx 3.5\text{-pA Cs}^+$ primary beam was focused to a nominal spot size of $\approx 100\text{ nm}$ and rastered

over the sample in 32×32 , 64×64 , or 128×128 -pixel arrays to generate secondary ions. The dwell time was 2–5 ms/pixel, and the raster size was varied from 1×1 to $4 \times 4\ \mu\text{m}^2$, depending on the dimensions of the area to be analyzed. The secondary ion mass spectrometer was tuned for a mass resolving power of $\approx 6,800$ to resolve isobaric interferences. Negative secondary ions ($^{12}\text{C}^-$, $^{13}\text{C}^-$, $^{12}\text{C}^{14}\text{N}^-$, and $^{12}\text{C}^{15}\text{N}^-$) were detected in simultaneous collection mode by pulse counting to generate 20–80 serial quantitative secondary ion images (i.e., layers). A normal incidence electron flood gun was used for charge compensation. There were two sets of measurements: (i) the $\delta^{13}\text{C}$ value reported above comes from measurements of C and N isotope abundances on the uncoated foils; (ii) because of the low intensity of CN^- ions, a $\approx 25\text{-nm}$ -thick carbon coat was deposited onto the foil to compensate for the low abundance of C in the TiN and maximize the formation of CN^- secondary ions. With this procedure, the $^{12}\text{C}^{14}\text{N}^-$ intensity increased substantially to $\approx 500,000\ \text{s}^{-1}$ at the onset of each analysis. The data were corrected for instrumental mass-dependent fractionation of C and N based on analyses of National Institute of Standards and Technology (NIST) SRM-8558 (potassium nitrate) mixed with NIST SRM-8541 (graphite) and *Bacillus subtilis* endospore samples of known $\delta^{13}\text{C}$ and $\delta^{15}\text{N}$ (39). The difference in chemical composition between the C-rich nitrogen isotope standards and the Ti-rich, C-poor TiN raises a potential concern over the accuracy of the mass-dependent fractionation correction. Although a full evaluation requires a TiN standard with well-determined $^{15}\text{N}/^{14}\text{N}$, the absence of significant variations in instrumental mass-dependent fractionation for a variety of N-bearing materials supports the approach followed here. Data were processed as quantitative isotopic ratio images by using custom software (L'image; L. Nittler, Lawrence Livermore National Laboratory) and were corrected for detector dead time and image shift from layer to layer. Regions of interest (ROIs) were defined based on elemental composition correlated with TEM imaging of the FIB sections, and the isotopic composition for each ROI was calculated by averaging over the replicate layers.

ACKNOWLEDGMENTS. We thank W. Heinrich (GeoForschungsZentrum Potsdam), A. Navrotsky (University of California, Davis), and A. El Goresy (Bayreuth Geoinstitute, Bayreuth, Germany) for discussions of nitrogen significance for Earth's deep interior; L. Nittler for assistance with image processing; and two anonymous reviewers for their fruitful comments on the manuscript. This work was supported by the Chinese National Science Foundation (to J.Y.) and a GeoForschungsZentrum travel grant (to L.F.D.). L.F.D.'s research was partly supported by University of California Lab Fees Research Program Grant 09-LR-05-116946DOBL.

- Haggerty SE, Sautter V (1990) Ultra-deep (greater than 300-km ultramafic upper mantle xenoliths. *Science* 248:993–996.
- Dobrzhinetskaya LF, Green HW, Wang S (1996) Alpe-Arami: A peridotite massif from depth of more than 300 kilometers. *Science* 271:1841–1845.
- Liou JG, Zhang RY, Ernst GW (2007) Very high-pressure orogenic garnet peridotites. *Proc Natl Acad Sci USA* 104:9116–9121.
- Liu X-W, Jin Z-M, Green HW (2007) Clinostatite exsolution in diopsidic augite of Dabieshan: Garnet peridotite from depth of 300 km. *Am Mineral* 92:546–552.
- Spengler D, et al. (2006) Deep orogen and hot melting of an Archaean orogenic peridotite massif in Norway. *Nature* 440:913–917.
- Liu L, Zhang J, Green HW, Jin ZM, Bozhilov KN (2007) Evidence of former stishovite in metamorphosed sediments, implying subduction to $>350\text{ km}$. *Earth Planet Sci Lett* 263:180–191.
- Kaminsky FV, et al. (2001) Superdeep diamonds from the Juina area, Mato Grosso State, Brazil. *Contrib Mineral Petrol* 140:734–753.
- Yang JS, et al. (2007) Diamond- and coesite-bearing chromitites from the Luobusa ophiolite, Tibet. *Geology* 35:875–878.
- Yamamoto S, Komiya T, Hirose K, Maruyama S (2009) Coesite and clinopyroxene exsolution lamellae in chromites: In situ ultrahigh-pressure evidence from podiform chromitites in the Luobusa ophiolite, southern Tibet. *Lithos* 109:314–322.
- Yang JS, et al. (2007) Diamond and unusual minerals discovered from the chromitite in Polar Ural: A first report. *Eos Trans AGU Fall Meeting Suppl* 88:V43E-05.
- Matveev S, Ballhaus C (2002) Role of water in the origin of podiform chromitite deposits. *Earth Planet Sci Lett* 203:235–243.
- Robinson PT, et al. (2004) In *Aspects of the tectonic evolution of China*, eds Malpas J, Fletcher CJ, Aitchison JC, Ali J (Geological Society, London), Vol 226, pp 247–272.
- Aitchison JC, et al. (2002) New insights into the evolution of the Yarlung Tsangpo suture zone, Xizang (Tibet), China. *Episodes* 25:90–94.
- Xu XZ, et al. (2009) Unusual mantle mineral group from chromitite ore body Cr-11 in Luobusa Ophiolite of Yarlung-Zangbo Suture Zone, Tibet. *J Earth Sci* 20:284–302.
- Withers AC, Essene EJ, Zhang Y (2003) Rutile/TiO₂ phase equilibria. *Contrib Mineral Petrol* 145:199–204.
- Tatarintsev VI, Sandomirskaya SM, Tsumbal SN (1987) First discovery of titanium nitride (osbornite) in terrestrial rocks. *Dokl Russ Akad Nauk* 296:1458–1461.
- Parthasarathy G, Haggerty SE, Kunvar AC (2005) Nano-crystalline osbornite from Carbonados: Spectroscopic studies. *Geochim Cosmochim Acta* 69:A521.
- Meibom A, Krot AN, Robert F, Mostefa S (2007) Nitrogen and carbon isotopic composition of the sun inferred from a high-temperature solar nebular condensate. *Astrophys J* 656:L33–L36.
- Hwang SL, Shen PY, Chu HT, Yui TF (2001) Nanometer-size $\alpha\text{-PbO}_2$ -type TiO₂ in garnet: A thermobarometer for ultrahigh-pressure metamorphism. *Science* 288:321–324.
- Wu XL, Meng DW, Han YJ (2005) $\alpha\text{-PbO}_2$ -type nanophase TiO₂ from coesite-bearing eclogite in the Dabie Mountains, China. *Am Mineral* 90:1458–1461.
- Frost DJ, et al. (2004) Experimental evidence for the existence of iron-rich metal in the Earth's lower mantle. *Nature* 428:409–412.
- McCammon CA (2005) The paradox of mantle redox. *Science* 308:807–808.
- Rohrbach A, et al. (2007) Metal saturation in the upper mantle. *Nature* 449:456–458.
- Sekine T, He H, Kobayashi T, Shibata K (2006) Sinoite (S₂N₂O) shocked at pressures of 28 to 64 GPa. *Am Mineral* 91:463–466.
- Dubrovinskaya N, et al. (2007) Suprhard nanocomposite of dense polymorphs of boron nitride: Noncarbon material has reached diamond hardness. *Appl Phys Lett* 90:10192–10195.
- Chen M, Shu J, Mao HK, Xie X, Hemley RJ (2003) Natural occurrence and synthesis of two new postspinel polymorphs of chromite. *Proc Natl Acad Sci USA* 100:14651–14654.
- Woodland AB, Angel RJ (2000) Phase relations in the system fayalite-magnetite at high pressures and temperatures. *Contrib Mineral Petrol* 139:734–747.
- Ono S, Hirose K, Murakami M, Ishiki M (2002) Poststishovite phase boundary in SiO₂ determined by in situ X-ray observations. *Earth Planet Sci Lett* 197:187–192.
- Setaka N, Sato T (1992) In *Shock Compression Technology and Materials Science*, ed Sawaoka AB (KTK Scientific Publisher/Terra Scientific Publishing Company, Tokyo), pp 87–102.
- Liu X, et al. (2006) Decomposition of kyanite and solubility of Al₂O₃ in stishovite at high-pressure and high-temperature conditions. *Phys Chem Miner* 33:711–721.
- Marty B, Dauphas N (2003) The nitrogen record of crust–mantle interaction and mantle convection from Archean to present. *Earth Planet Sci Lett* 206:397–410.
- Cartigny P, Boyd S, Harris J, Javoy M (1997) Nitrogen isotopes in peridotitic diamonds from Fuxian, China: The mantle signature. *Terra Nova* 9:175–179.
- Javoy M (1998) The birth of the Earth's atmosphere: The behavior and fate of its major elements. *Chem Geol* 147:11–15.

34. Mathez EA, Fogel RA, Hutcheon ID, Marshintsev VK (1995) Carbon isotopic composition and origin of SiC from kimberlites of Yakutia, Russia. *Geochim Cosmochim Acta* 59:781–791.
35. Madiba CCP, Pollak H, Cawthorn RG, Viljoen F (1998) Ilmenite: Mantle reservoir for nitrogen? *Hyperfine Interact* 111:319–327.
36. Adler JF, Williams Q (2005) A high-pressure X-ray diffraction studies of iron nitrides: Implication for Earth's core. *J Geophys Res* 110:B011203.1–B011203.15.
37. Cartigny P, Jendrzejewski A, Pineau NF, Petit E, Javoy M (2001) Volatile (C, N, Ar) variability in MORB and the respective roles of mantle source heterogeneity and degassing: The case of the Southwest Indian Ridge. *Earth Planet Sci Lett* 194:241–257.
38. Wirth R (2004) Focused ion beam (FIB): A novel technology for advanced application of micro- and nanoanalysis in geosciences and applied mineralogy. *Eur J Mineral* 16:863–876.
39. Kreuzer-Martin HW, Jarman KH (2007) Stable isotope ratios and forensic analysis of microorganisms. *Appl Environ Microbiol* 73:3896–3907.